Absolute Measurement of the Relativistic Magnetic Dipole Transition Energy in Heliumlike Argon

Pedro Amaro,[1,2] Sophie Schlesser,[1,*] Mauro Guerra,[2] Eric-Olivier Le Bigot,[1] Jean-Michel Isac,[1] Pascal Travers,[1] José Paulo Santos,[2] Csilla I. Szabo,[1] Alexandre Gumberidze,[1,3,4] and Paul Indelicato[1,†]

[1]*Laboratoire Kastler Brossel, Ecole Normale Supérieure, CNRS, Université Pierre et Marie Curie-Paris 6, Case 74, 4 Place Jussieu, F-75005 Paris, France*

[2]*Centro de Física Atómica, CFA, Departamento de Física, Faculdade de Ciências e Tecnologia, FCT, Universidade Nova de Lisboa, 2829-516 Caparica, Portugal*

[3]*ExtreMe Matter Institute EMMI and Research Division, GSI Helmholtzzentrum für Schwerionenforschung, D-64291 Darmstadt, Germany*

[4]*Frankfurt Institute for Advanced Studies FIAS, D-60438 Frankfurt am Main, Germany*

(Received 31 May 2011; published 27 July 2012)

The $1s2s\ ^3S_1 \rightarrow 1s^2\ ^1S_0$ relativistic magnetic dipole transition in heliumlike argon, emitted by the plasma of an electron-cyclotron resonance ion source, has been measured using a double-flat crystal x-ray spectrometer. Such a spectrometer, used for the first time on a highly charged ion transition, provides absolute (reference-free) measurements in the x-ray domain. We find a transition energy of 3104.1605(77) eV (2.5 ppm accuracy). This value is the most accurate, reference-free measurement done for such a transition and is in good agreement with recent QED predictions.

DOI: 10.1103/PhysRevLett.109.043005 PACS numbers: 31.30.J−, 12.20.Fv, 32.30.Rj

Detailed tests of bound-state quantum electrodynamics are provided by simple systems like hydrogen, in which transitions to the $1s$ level have been measured with an accuracy of a few parts in 10^{14} [1,2] while the $n = 2$ Lamb shift is known to a few ppm accuracy [3]. Helium has been studied [4] and agreement between experiment [5,6] and theory [7] in the fine structure is now very good. Yet, a recent measurement of the Lamb shift in muonic hydrogen (μp) [8] provides a proton charge radius 6.9σ away from the 2010 CODATA value [9] obtained by combining results from hydrogen spectroscopy and electron-proton scattering [10]. Investigations using systems with different scales compared to the electron Compton wavelength $\lambda_C = 386.159 \times 10^{-15}$ m (the fundamental scale of QED), different field strengths as measured by $Z\alpha$ (Z is the atomic number and $\alpha \approx 1/137$ the fine structure constant), and different nuclear size corrections are required to provide stringent tests of bound-state QED and to explore possible causes for this discrepancy.

One- and two-electron highly-charged ions provide sensitive tests of bound-state QED, which vary as $(Z\alpha)^4$ while the dominant nonrelativistic contribution to the transition energy varies like $(Z\alpha)^2$. They allow us to explore a wide range of Bohr radii to Compton wavelength ratios $r_B/\lambda_C \approx m_e n^2/(m_\mu \alpha Z)$. For the $2s$ Lamb-shift in μp, it is ≈ 2.9. For the $1s$ shell this ratio ranges from 137 at $Z = 1$ to 7.5 at $Z = 18$, 2.9 at $Z = 44$ (identical to μp) and 1.1 at $Z = 92$, taking into account relativistic corrections. Yet, for the $n = 2$ shell, this ratio is still 4.1 at $Z = 92$. The impact of the main QED corrections are quite different: while the vacuum polarization is 100.3% of the $2s$ Lamb-shift in μp, it represents only -2.6% for the $1s$ shell for H, -7.6% for Ar, and -35.4% for U. The finite size correction varies like $\approx Z^{14/3}$. All these corrections can be better understood by doing accurate measurements on a wide range of atomic numbers in HCI and muonic atoms [11].

A number of accurate experiments have been performed on the $1s^2 2p \rightarrow 1s^2 2s$ transition in lithiumlike ions up to uranium [12,13]. These measurements have accuracies of the order of the size of two-loop QED corrections to the lower level energy [14]. Such $\Delta n = 0$ transitions have also been measured in two-electron Si^{12+} with laser spectroscopy to 0.8 ppm [15] and in U^{90+} [16]. Measurements of $n = 2 \rightarrow n = 1$ transitions, even at high-Z, are not yet sufficiently accurate to test two-loop QED corrections [17]. Very high-Z systems are also very sensitive to nuclear size corrections (see, e.g., [18]) and nuclear polarization [19], which ultimately limits the accuracy of the comparison. The allowed $1s2p\ ^1P_1 \rightarrow 1s^2$ transition in He-like argon has been measured to 1.9 ppm accuracy, relative to the theoretical value of the Lyman α transition in H-like argon [20], and to 1.5 ppm without external reference [21]. Earlier absolute measurements on both the $M1$ and $1s2p \rightarrow 1s^2$ transitions of He-like V [22], were calibrated against a series of x-ray standards [23,24], reaching an accuracy of ≈ 30 ppm. Half of this uncertainty is associated with the difficulties associated with x-ray standards mentioned above. In beam-foil spectroscopy, the in-beam calibration technique, which compares Lyman and Balmer lines in first and second orders, yields accuracies of 34 ppm on H-like iron [25] and 15 ppm on H-like Ge [26]. In the present work, we have used a double-crystal spectrometer and an electron-cyclotron resonance ion source (ECRIS) to perform a 2.5 ppm measurement of

the $1s2s\,^3S_1 \rightarrow 1s^2\,^1S_0$ relativistic $M1$ transition in He-like argon, without reference to any theoretical or experimental energy, using the known lattice spacing of a Si crystal, tied to the definition of the meter, as a transfer standard. This method avoids the difficulties associated with existing x-ray standards from core-excited neutral elements, such as broad, asymmetric lines and sensitivity to excitation conditions and chemical effects [23,24].

We have built a reflection vacuum double-crystal spectrometer [27] (Fig. 1) for this measurement. Up to now, such an instrument was only used to perform a few absolute energy measurements on core-excited light neutral atoms from Mg [28] to K [29], several unpublished (see Ref. [24]), with accuracies of a few ppm. In this device, the first crystal, kept at a fixed angle, acts as a collimator, defining the direction of the incoming x-ray beam, which is analyzed by the second crystal. A first peak is obtained by scanning the second crystal angle when the two crystals are parallel (nondispersive mode). The peak shape depends only on the crystal reflection profile and provides the instrument response function. A second peak is obtained when both crystals deflect the beam in the same direction (dispersive mode). The peak shape is then a convolution of the line shape and of the instrument response function. The position of the first crystal is the same in both modes. The difference in angle settings of the second crystal between the nondispersive and the dispersive modes is directly connected to the Bragg angle. The spectrometer is built for mechanical and thermal stability and precision positioning of the crystals. The rotation angle of the first crystal is measured by an optical encoder, which allows monitoring and maintaining the position of the axis to better than 0.07''. The second axis angle is measured with an accuracy of 0.2'' (1.2 ppm at 3.1 keV.) A third rotation table, concentric to the second crystal axis, allows positioning of the x-ray detector.

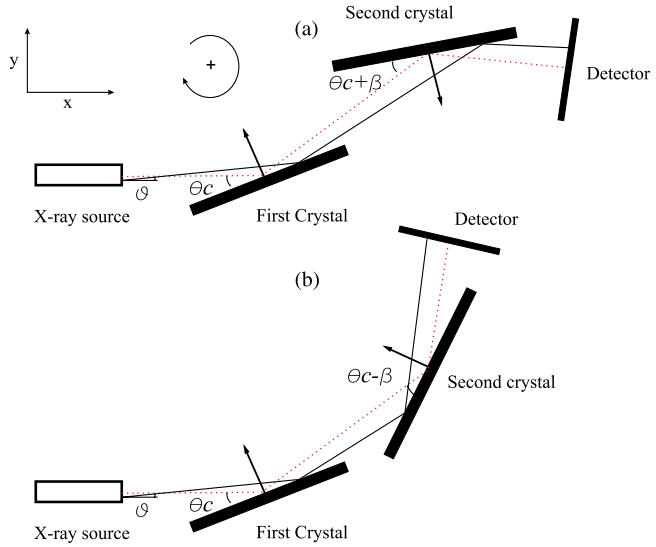

FIG. 1 (color online). Schematic of the spectrometer and ECRIS (not to scale). (a) nondispersive mode. (b) dispersive mode. The dotted line represents the optical axis of the instrument. The crystals are 6 mm thick. The plasma-first crystal distance is 1.4 m and the distance between the two axes is 42 cm.

The two 6×4 cm^2, 6-mm thick Si(111) crystals were made at NIST. Their lattice spacing in vacuum was found to be $d = 3.135\,601\,048(38)$ Å (0.012 ppm) at a temperature of 22.5 °C [10,30,31]. Our measurement provides a wavelength directly tied to the definition of the meter [10,32]. The dilatation coefficient provided by NIST is 2.56×10^{-6} °C^{-1}. To reduce the effect of asymmetric reflection, the crystals were polished then etched in such a way that the angle between the surface and x-ray planes is smaller than 11''. The etching is required to avoid line broadening due to damages of the crystal surface. The temperature of the crystals is measured and controlled to better than 0.2 °C. To account for possibly bad thermal contacts under vacuum, and front-to-back temperature differences, we use a final uncertainty of 0.5 °C.

The x-ray spectrometer is connected to the ECRIS in such a way that the first crystal is located at 1.2 m from the center of the plasma (a sphere of ≈ 3 cm in diameter). The axis of the spectrometer is aligned on the ECRIS axis with a telescope and a laser to a precision of 0.01°. The different apertures located between the source and the first crystal limit the x-ray beam diameter to 1.2 cm. The plasma position and diameter are very stable, as they are imposed by the magnetic field structure.

The experiment was performed on a 14.5 GHz ECRIS, fully characterized for x-ray production [33]. In an ECRIS, the electrons are trapped by the magnetic field, and the ions by the space charge of the electrons, which have a density around 10^{11} cm^{-3}. This corresponds to a trapping potential of a fraction of a volt, leading to a Doppler broadening of the observed $M1$ transition. The natural width of this transition is $\approx 10^{-7}$ eV [34,35], compared to ≈ 1 eV for neutral Ar x rays. Even with Doppler broadening, it is much narrower than the instrument response function. We can, thus, directly

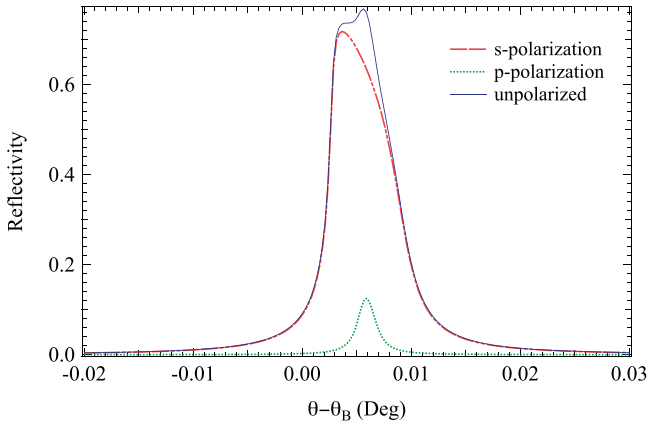

FIG. 2 (color online). Reflectivity profile of a Si(111) crystal for an x-ray energy equal to 3104.148 eV, calculated with XOP [36].

probe for the first time the shape of this response function in both dispersive and nondispersive mode. To analyze the experimental spectra, we developed a simulation code, that does an exact ray tracing using the geometry of the instrument and of the x-ray source, the shape of the crystal reflectivity profile, as well as the linewidth and Gaussian Doppler broadening. The effect of the x-ray beam vertical divergence and of the Si index of refraction are then described exactly and not by a formula as in previous work. The reflectivity profile on Fig. 2 is calculated using the XOP program [36], which uses dynamical diffraction theory from [37]. The result was checked with X0H [38,39]. The index of refraction in XOP at 3104.148 eV is 5.100×10^{-5}. The semiempirical value from Ref. [40] is 5.079×10^{-5}. We use this difference as an error bound for this correction. A detailed description of the instrument, the simulation, and the alignment procedure can be found in [31].

A spectrum obtained in the nondispersive mode is shown in Fig. 3. The fit was performed with a Voigt profile and a simulated profile. Both fits give the same peak position. The simulation reproduces the profile with a reduced $\chi^2 \approx 1.2$, showing the near perfect quality of the crystals. The observation of an additional broadening on the dispersive side must then come from the Doppler effect. Here, because of the slight asymmetry of the real profile, a small shift between the results obtained from simulation or Voigt profile is observed, that translates into a 14 meV (4.6 ppm) energy shift. To our knowledge, this is the first time that such a shift is observed and it has never been taken into account in previous standards measurements reported in the latest x-ray energy tables [24]. We find a Doppler broadening of 80.5(4.6) meV (FWHM) by averaging the Gaussian width obtained by fitting all 13 recorded spectra with simulated profiles corresponding to different widths and minimizing the χ^2 [31].

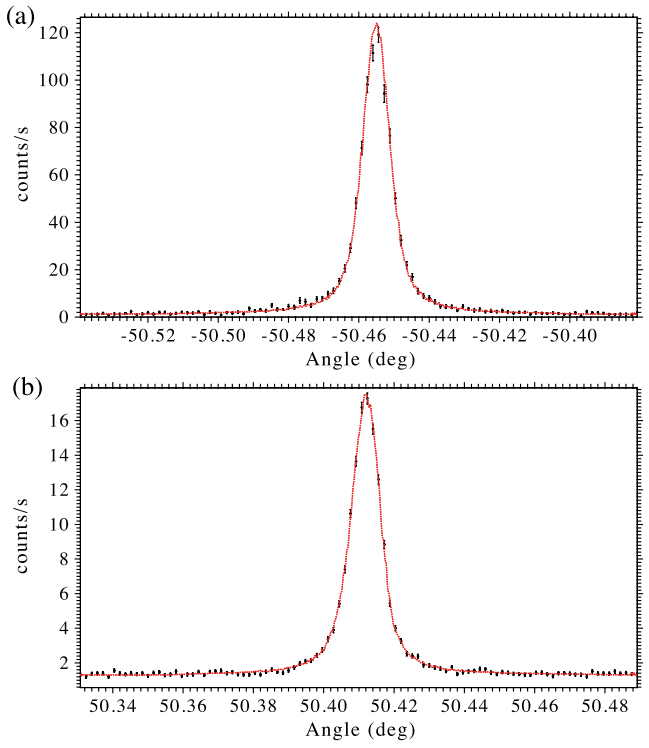

FIG. 3 (color online). (a) Spectrum obtained with the spectrometer in the nondispersive position (acquisition time 943 s), fitted with an *ab initio* simulated profile (only position and intensity are adjusted). As expected, the quality of the fit (reduced $\chi^2 \approx 1.2$) does not depend on the line spectral shape (i.e., the width of the Gaussian broadening). (b) Spectrum of the $M1$ transition obtained in the dispersive mode (acquisition time 18 239 s), fitted with the simulated profile using the Gaussian Doppler broadening as an additional fit parameter. A reduced $\chi^2 \approx 0.75$ is obtained for the optimal Gaussian broadening.

In order to study systematic errors, a series of spectra were recorded over a period of several months, at different temperatures, with slightly different first crystal angles and ECRIS operating conditions. The microwave power, gas composition, and ion extraction voltage were varied to check their influence on the line energy. No dependence on the first crystal angle or ECRIS parameters was observed.

Two analyses were performed on the x-ray spectra. A Voigt profile was fitted to the dispersive and nondispersive spectra, as well as to high statistic simulated spectra. The experimental energy was then deduced from the energy used as an input for the simulation corrected for the difference in angle and temperature. In a second method, the simulated profiles are directly used to fit the experimental lines and obtain a Bragg angle from which the line energy was deduced. Both methods provide the same result to high accuracy. The dependence of the measured transition energy on temperature is shown on Fig. 4. Weighted one- and two-parameter linear fits have been performed. The difference between the values at 22.5 °C obtained with those fits

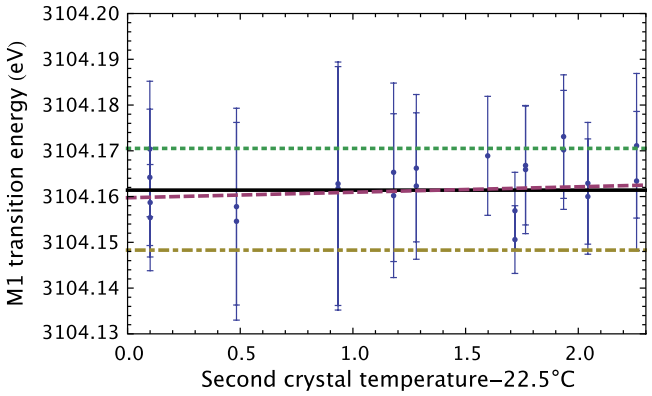

FIG. 4 (color online). One- and two-parameter extrapolation of the $M1$ transition energy to the standard temperature (22.5 °C). Each data point corresponds to the energy deduced from a one-day measurement, a sequence of three spectra like the ones in Fig. 3, performed successively in dispersive, nondispersive, and dispersive mode, for a given temperature. The error bars correspond to the statistical errors from the fits. Dot-dashed line: Ref. [41]. Dotted line: MCDF calculation (see Table II).

TABLE I. Contributions to the uncertainty on the $M1$ transition energy measurement (68% confidence interval).

Contribution	Value (eV)
Fit and extrapolation	0.0044
Angle encoder error	0.0036
Temperature (0.5 °C)	0.0040
Crystal tilts ($\pm$ 0.01° for each crystal)	0.0002
Vertical misalignment of collimators (1 mm)	0.0002
X-ray source size (6 to 12 mm)	0.0013
Form factors	0.0020
X-ray polarization	0.0014
Lattice spacing error	0.0001
Index of refraction	0.0016
Coefficient of thermal expansion	0.0002
Energy-wavelength correction	0.0001
Total	0.0077

are combined to get an estimate of systematic errors. Contributions to the uncertainty are shown in Table I. The uncertainty is limited by statistics, angle and temperature measurements. Possible contamination from satellite transitions, originating from $1s2sn\ell$, $n > 2$ levels must be low: some satellite lines should be resolved and seen outside of the $M1$ line, yet none can be observed. This is because the $n\ell$ electron decays by $E1$ transitions faster than the $2s$ one.

The final value for the $M1$ transition energy is 3104.1605 (77) eV (2.5 ppm). The comparison with theoretical results is shown in Table II. The theoretical result of Artemyev *et al.* [41] is 1.6σ below the experimental value. The contributions included in [41] and their uncertainty are also shown in Table II. Our experimental accuracy is 0.7% of the one-electron QED corrections, and 7.4% of the self-energy correction to the electron-electron interaction. The finite size correction represents 2.7 ppm of the transition energy, barely larger than our uncertainty. Its uncertainty cannot influence the comparison between theory and experiment.

TABLE II. Comparison between theoretical calculations and experiment (eV). Individual contributions are from [41]. Older calculations are updated for fundamental constants [10]. The multiconfiguration Dirac-Fock (MCDF) calculation follows Refs. [42,43].

Contribution	$1s^2\ {}^1S_0$	$1s2s\ {}^3S_1$	Transition
Dirac	−4427.4154(3)	−1108.0563	3319.3591(3)
$\Delta E_{\rm int}$	305.6560	91.3873	−214.2687
$\Delta E_{\rm 1el}^{\rm QED}$	1.1310(1)	0.1525	−0.9785(1)
$\Delta E_{\rm 2el}^{\rm QED}$:			
Scr. SE	−0.1116	−0.0154	0.0962
Scr. VP	0.0072	0.0010	−0.0062
2-ph.exch.	0.0091(1)	−0.0004(1)	−0.0095(2)
$\Delta E_{\rm ho}^{\rm QED}$	0.0009	0.0003	−0.0006
$\Delta E_{\rm rec}$	0.0575	0.0141	−0.0434
Total [41]	−4120.6653(4)	−1016.5169(1)	3104.1484(4)
MCDF [44]			3104.171
Drake [45]			3104.138
RMBPT [46]			3104.189
RMBPT [34]			3104.06(19)
Experiment			3104.1605(77)

In conclusion, we have performed a very accurate measurement of an x-ray transition energy in HCI, without the need for any external or theoretical energy reference. This has been achieved using a high-precision x-ray double-crystal spectrometer, which was made possible thanks to the very intense emission of the $M1$ transition from the ECRIS plasma. Our measurement provides an experimental test of QED at a distance scale 3 times larger than in the case of muonic hydrogen. The QED contribution (Table II) is tested with an accuracy of 0.8%, while the discrepancy observed for the Lamb shift in μP is 0.2%.

We have been able to demonstrate by using a very narrow line and *ab initio* simulations that our spectrometer reaches theoretical performances. We proved from the $M1$ broadening that the ions in the ECRIS are colder than expected. We have established the first x-ray standard based on a narrow, symmetric line that can be used to calibrate any instrument in this energy range to our quoted accuracy, without the problems associated with previous, x-ray tubes based standards.

With this system we can now investigate core-excited ions with 3 and 4 electrons to study correlation and Auger shifts. Thanks to the well understood line shape of the double-crystal spectrometer, it will be possible to obtain the intrinsic width of these transitions to a few percent accuracy. This will allow us to study radiative and Auger contributions to the transition probability. In the future, with the use of a higher performance ECRIS (larger plasma and higher electronic densities), improvements in the temperature controls and angle measurements accuracy of the double-crystal spectrometer [47], it will be possible to obtain x-ray energies with an accuracy below 1 ppm and to perform measurements on heavier elements.

Laboratoire Kastler Brossel is "UMR No. 8552" of the ENS, CNRS, and UPMC. Our ECRIS has been financed by grants from CNRS, MESR, and UPMC. The experiment is supported by grants from BNM No. 01 3 0002, the ANR No. ANR-06-BLAN-0223, the Helmholtz Alliance No. HA216/EMMI, the FCT (PTDC/FIS/117606/2010 and PEst-OE/FIS/UI0303/2011, CFA), the PESSOA Program No. 441.00, the Acções Integradas Luso-Francesas No. F-11/09, and the Programme Hubert Curien PESSOA No. 20022VB. P. A. and M. G. acknowledge the support of the FCT, Contracts No. SFRH/BD/37404/2007 and No. SFRH/BD/38691/2007. We thank J. P. Okpisz, B. Delamour, M. Boujrad, A. Vogt, and S. Souramassing for technical support and the ASUR team from INSP. We thank A. Henins and E. Kessler for preparing and measuring the crystals and L. Hudson, J. Gillaspy, and T. Jach for helpful discussions.

*Present address: KVI, Theory Group, University of Groningen, 9747 AA Groningen, The Netherlands.
†paul.indelicato@lkb.ens.fr

[1] M. Niering, R. Holzwarth, J. Reichert, P. Pokasov, T. Udem, M. Weitz, T. W. Hänsch, P. Lemonde, G. Santarelli, M. Abgrall, P. Laurent, C. Salomon, and A. Clairon, Phys. Rev. Lett. **84**, 5496 (2000).
[2] C. G. Parthey, A. Matveev, J. Alnis, B. Bernhardt, A. Beyer, R. Holzwarth, A. Maistrou, R. Pohl, K. Predehl, T. Udem, T. Wilken, N. Kolachevsky, M. Abgrall, D. Rovera, C. Salomon, P. Laurent, and T. W. Hänsch, Phys. Rev. Lett. **107**, 203001 (2011).
[3] B. de Beauvoir, C. Schwob, O. Acef, L. Jozefowski, L. Hilico, F. Nez, L. Julien, A. Clairon, and F. Biraben, Eur. Phys. J. D **12**, 61 (2000).
[4] D. Z. Kandula, C. Gohle, T. J. Pinkert, W. Ubachs, and K. S. E. Eikema, Phys. Rev. Lett. **105**, 063001 (2010).
[5] J. S. Borbely, M. C. George, L. D. Lombardi, M. Weel, D. W. Fitzakerley, and E. A. Hessels, Phys. Rev. A **79**, 060503 (2009).
[6] M. Smiciklas and D. Shiner, Phys. Rev. Lett. **105**, 123001 (2010).
[7] K. Pachucki and V. A. Yerokhin, Phys. Rev. Lett. **104**, 070403 (2010).
[8] R. Pohl *et al.*, Nature (London) **466**, 213 (2010).
[9] CODATA, "Internationally Recommended Values of the Fundamental Physical Constants 2010," http://physics.nist.gov/cuu/Constants/index.html.
[10] P. J. Mohr, B. N. Taylor, and D. B. Newell, Rev. Mod. Phys. **80**, 633 (2008).
[11] A. Antognini *et al.*, Can. J. Phys. **89**, 47 (2011).
[12] C. Brandau, C. Kozhuharov, A. Müller, W. Shi, S. Schippers, T. Bartsch, S. Böhm, C. Böhme, A. Hoffknecht, H. Knopp, N. Grün, W. Scheid, T. Steih, F. Bosch, B. Franzke, P. H. Mokler, F. Nolden, M. Steck, T. Stöhlker, and Z. Stachura, Phys. Rev. Lett. **91**, 073202 (2003).
[13] P. Beiersdorfer, H. Chen, D. B. Thorn, and E. Träbert, Phys. Rev. Lett. **95**, 233003 (2005).
[14] P. Beiersdorfer, J. Phys. B **43**, 074032 (2010).
[15] T. R. DeVore, D. N. Crosby, and E. G. Myers, Phys. Rev. Lett. **100**, 243001 (2008).
[16] M. Trassinelli, A. Kumar, H. F. Beyer, P. Indelicato, R. Märtin, R. Reuschl, Y. S. Kozhedu, C. Brandau, H. Bräuning, S. Geyer, A. Gumberidze, S. Hess, P. Jagodzinski, C. Kozhuharov, D. Liesen, S. Trotsenko, G. Weber, D. F. A. Winters, and T. Stöhlker, Europhys. Lett. **87**, 63001 (2009).
[17] A. Gumberidze, T. Stöhlker, D. Banaś, K. Beckert, P. Beller, H. F. Beyer, F. Bosch, S. Hagmann, C. Kozhuharov, D. Liesen, F. Nolden, X. Ma, P. H. Mokler, M. Steck, D. Sierpowski, and S. Tashenov, Phys. Rev. Lett. **94**, 223001 (2005).
[18] S. Fritzsche, P. Indelicato, and T. Stöhlker, J. Phys. B **38**, S707 (2005).
[19] G. Plunien, B. Muller, W. Greiner, and G. Soff, Phys. Rev. A **43**, 5853 (1991).
[20] H. Bruhns, J. Braun, K. Kubiček, J. R. Crespo Lopez-Urrutia, and J. Ullrich, Phys. Rev. Lett. **99**, 113001 (2007).
[21] K. Kubiček, J. Braun, H. Bruhns, J. R. C. Lopez-Urrutia, P. H. Mokler, and J. Ullrich, Rev. Sci. Instrum. **83**, 013102 (2012).
[22] C. T. Chantler, D. Paterson, L. T. Hudson, F. G. Serpa, J. D. Gillaspy, and E. Takacs, Phys. Rev. A **62**, 042501 (2000).
[23] D. F. Anagnostopoulos, D. Gotta, P. Indelicato, and L. M. Simons, Phys. Rev. Lett. **91**, 240801 (2003).
[24] R. Deslattes, E. Kessler, Jr., P. Indelicato, L. de Billy, E. Lindroth, and J. Anton, Rev. Mod. Phys. **75**, 35 (2003).
[25] C. T. Chantler, J. M. Laming, D. D. Dietrich, W. A. Hallett, R. McDonald, and J. D. Silver, Phys. Rev. A **76**, 042116 (2007).
[26] C. T. Chantler, J. M. Laming, J. D. Silver, D. D. Dietrich, P. H. Mokler, E. C. Finch, and S. D. Rosner, Phys. Rev. A **80**, 022508 (2009).
[27] R. D. Deslattes, Rev. Sci. Instrum. **38**, 616 (1967).
[28] J. Schweppe, R. D. Deslattes, T. Mooney, and C. J. Powell, J. Electron Spectrosc. Relat. Phenom. **67**, 463 (1994).
[29] R. D. Deslattes and J. E. G. Kessler, in *Atomic Inner-Shell Physics*, edited by B. Crasemann (Plenum, New York, 1985), pp. 181–235.
[30] E. G. Kessler, A. Henins, R. D. Deslattes, L. Nielsen, and M. Arif, J. Res. Natl. Inst. Stand. Technol. **99**, 1 (1994).
[31] P. Amaro, C. I. Szabo, S. Schlesser, A. Gumberidze, J. E. G. Kessler, A. Henins, E.-O. L. Bigot, M. Trassinelli, J.-M. Isac, P. Travers, M. Guerra, J.-P. Santos, and P. Indelicato, arXiv:1205.4520.
[32] H. Fujimoto, A. Waseda, and X. W. Zhang, Metrologia **48**, S55 (2011).
[33] A. Gumberidze, M. Trassinelli, N. Adrouche, C. I. Szabo, P. Indelicato, F. Haranger, J.-M. Isac, E. Lamour, E.-O. L. Bigot, J. Merot, C. Prigent, J.-P. Rozet, and D. Vernhet, Rev. Sci. Instrum. **81**, 033303 (2010).
[34] E. Lindroth and S. Salomonson, Phys. Rev. A **41**, 4659 (1990).
[35] P. Indelicato, Phys. Rev. Lett. **77**, 3323 (1996).
[36] M. Sanchez del Rio and R. J. Dejus, in *Proceedings of SPIE-International Society for Optical Engineering* (SPIE, Bellingham, WA, 2004), pp. 171–174.
[37] W. H. Zachariasen, *Theory of X-ray Diffraction in Crystals* (John Wiley and Sons, New York, 1945).
[38] S. Stepanov, "X0H on the Web," http://sergey.gmca.aps.anl.gov/x0h.html.
[39] O. M. Lugovskaya and S. A. Stepanov, Sov. Phys. Crystallogr. **36**, 478 (1991).
[40] B. L. Henke, E. M. Gullikson, and J. C. Davis, At. Data Nucl. Data Tables **54**, 181 (1993).
[41] A. N. Artemyev, V. M. Shabaev, V. A. Yerokhin, G. Plunien, and G. Soff, Phys. Rev. A **71**, 062104 (2005).
[42] P. Indelicato, O. Gorceix, and J. P. Desclaux, J. Phys. B **20**, 651 (1987).
[43] P. Indelicato, Nucl. Instrum. Methods Phys. Res., Sect. B **31**, 14 (1988).
[44] P. Indelicato (unpublished).
[45] G. W. F. Drake, Nucl. Instrum. Methods Phys. Res., Sect. B **31**, 7 (1988).
[46] D. R. Plante, W. R. Johnson, and J. Sapirstein, Phys. Rev. A **49**, 3519 (1994).
[47] W. T. Estler, J. Res. Natl. Inst. Stand. Technol. **103**, 141 (1998).